X-ray Diffraction from a Left Ventricular Wall of Rat Heart

Naoto Yagi,* Juichiro Shimizu,[†] Satoshi Mohri,[†] Jun'ichi Araki,[†] Kazufumi Nakamura,[†] Hiroshi Okuyama,[‡] Hiroko Toyota,[‡] Taro Morimoto,[†] Yuki Morizane,[†] Mie Kurusu,[†] Tatsushi Miura,[†] Katsushi Hashimoto,[†] Katsuhiko Tsujioka,[‡] Hiroyuki Suga,[¶] and Fumihiko Kajiya[†]

*SPring-8/JASRI, Sayo, Hyogo 679-5198, Japan; [†]Department of Cardiovascular Physiology, Okayama University Graduate School of Medicine and Dentistry, Shikata, Okayama 700-8558, Japan; [‡]Department of Physiology, Kawasaki Medical School, Matsushima, Kurashiki 701-0192, Japan; and [¶]National Cardiovascular Center Research Institute, Suita, Osaka 565-8565, Japan

ABSTRACT   We studied x-ray diffraction from the left ventricular wall of an excised, perfused whole heart of a rat using x rays from the third-generation synchrotron radiation facility, SPring-8. With the beam at right angles to the long axis of the left ventricle, well-oriented, strong equatorial reflections were observed from the epicardium surface. The reflections became vertically split arcs when the beam passed through myocardium deeper in the wall, and rings were observed when the beam passed into the inner myocardium of the wall. These diffraction patterns were explained by employing a layered-spiral model of the arrangement of muscle fibers in the heart. In a quiescent heart with an expanded left ventricle, the muscle fibers at the epicardium surface were found to have a (1,0) lattice spacing smaller than in the rest of the wall. The intensity ratio of the (1,0) and (1,1) equatorial reflections decreased on contraction with a similar time course in all parts of the wall. The results show that it is possible to assign the origin of reflections in a diffraction diagram from a whole heart. This study offers a basis for interpretation of x-ray diffraction from a beating heart under physiologically and pathologically different conditions.

INTRODUCTION

Owing to the high penetration power and short wavelength of x rays, the x-ray diffraction technique has been recognized as an important tool to study functions of cells at a molecular level nondestructively. This advantage has been utilized to study heart muscles over the last three decades (Matsubara, 1980). In most studies, a papillary or trabecular muscle was used as a specimen because of the good, parallel order of its muscle fibers.

In their pioneering work, Sowerby et al. (1994) recorded x-ray diffraction from a ventricular region of a whole rat heart during anoxic perfusion. They observed unoriented but strong equatorial reflections, indicating that oriented muscle fibers are not mandatory for an x-ray diffraction study on a heart. Changes in the x-ray equatorial reflections during a process of anoxia were successfully followed in their study.

It has been known that muscle fibers in a heart are arranged in such a way that their orientation changes continuously from endocardium to epicardium of the free wall. The myocardial wall can be regarded as a well-ordered, fiber-wound continuum of interconnecting muscle fibers in canine hearts (Streeter et al., 1969; Hsu et al., 1998; Hooks et al., 2002) (Fig. 1). Thus, x-ray diffraction from a whole heart is expected to consist of overlapping diffraction patterns from muscle fibers in various parts of the heart with different orientations through which the x-ray beam traverses. The diffraction pattern observed by Sowerby et al. (1994) was in fact an average of diffraction patterns from a large volume of a heart that was sampled by the cross section of the beam (5 mm horizontally, 1 mm vertically).

Compared with the second-generation synchrotron radiation source used by Sowerby et al. (1994), third-generation synchrotron radiation sources, such as SPring-8, are advantageous in the experiment on a whole heart for three reasons: 1), use of x rays with energies higher than those from the second-generation sources facilitates recording diffraction from a thick sample such as a rat heart; 2), higher flux makes it possible to follow changes in the diffraction pattern in a single heart beat with a high temporal resolution; and 3), a smaller x-ray beam is suitable for studying dynamics of a small part of a heart, e.g., epicardium, midcardium, and endocardium.

In this report, we show that, although the diffraction pattern from a whole heart is complex due to the transmural difference of muscle fiber orientation, it is possible to assign diffraction features to muscle fibers in most parts of the wall of a heart. Our experimental and theoretical study provides a basis for further functional studies on a whole heart using x-ray diffraction.

MATERIALS AND METHODS

Heart preparation

Male rats (Wistar, Japan Clea, Tokyo, Japan) 8 weeks of age were used. A rat was anaesthetized deeply with diethylether. Bilateral sternotomy was performed and the heart was rapidly excised and submerged in oxygenated, warmed modified Tyrode solution (136 mM NaCl, 5.4 mM KCl, 1.8 mM CaCl$_2$, 1.0 mM MgCl$_2$, and 5 mM HEPES, pH 7.3, at 25°C) containing 20 mM 2,3-butanedione monoxime (BDM) and 20 U/ml of heparin. The severed end of the aorta was fed over an 18-gauge blunted needle that was connected to a modified Langendorff perfusion system. The heart was perfused with the modified Tyrode solution containing 20 mM BDM without heparin to remove blood and stop beating. Perfusion pressure was
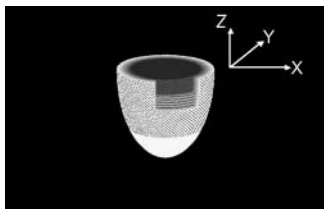
FIGURE 1 A simplified drawing model of the fiber orientation of the left ventricle with the right ventricle omitted for interpretation of complex x-ray diffraction patterns. In the epicardium, the fibers are inclined from the vertical z axis, which connects the base and apex. At the middle of the thickness of the wall, the fibers are running in the horizontal plane, and inclined in the opposite direction in the endocardium. The y axis is parallel to the x-ray beam, which runs horizontally. The horizontal section on the top is the ''equatorial'' plane, where the heart is widest, through which the x-ray beam passes into the heart.

set at ~100 mmHg. The animal experiments were conducted in accordance with the guidelines of SPring-8 for care and welfare of experimental animals.

The heart was set on the x-ray camera with the aorta pointing up, apex down, and the x-ray beam passing through the left ventricle from the anterior wall to the posterior wall. The height was adjusted so that the x-ray beam passed the equator of the heart (the equator is the vertical level where the heart is widest). The x-ray beam passed through the free wall of the left ventricle without passing through other parts of the heart.

When a quiescent heart was studied, it was perfused with the Tyrode solution containing 20 mM BDM from aorta. A water-filled thin latex balloon was inserted into the left ventricle and left ventricular volume was adjusted so that quiescent left ventricular pressure was ~10–20 mmHg. The total width of the diastolic arrested heart was ~12 mm, with the left ventricular free wall thickness ~2 mm. For x-ray scanning, the heart was moved horizontally at a constant speed of 1.0 mm/s. Since each frame was 212 ms (see below), the heart advanced by 0.212 mm in each frame, which is similar to the horizontal x-ray beam size (see below). The heart was kept perfused at 27°C. Tyrode solution always flowed over all surfaces of the heart.

To study a beating heart, complete heart block was achieved by formalin injection (10%, 0.1 ml) into the atrioventricular nodal region. The perfusate was changed to the Tyrode solution containing 2.2 mM Ca^{2+} without BDM. After recovery of spontaneous beats at sinus rhythm, the left atrium was opened and a thin latex balloon attached to an end of a stiff polyethylene tube was inserted into the left ventricle. The balloon and tube were filled with water and connected to a pressure transducer (Life Kit, Nihon Kohden, Tokyo, Japan) for measurement of left ventricular pressure during isovolumic contraction. The balloon volume was adjusted so that the end-diastolic left ventricular pressure was ~15 mmHg. A pair of pacing electrodes were placed on a right ventricular free wall. Then the heart was perfused with the oxygenated Tyrode solution without BDM and paced at 2 Hz. To prevent excessive movement, the heart was kept in a plastic tube with holes to pass x rays. To find the endocardial surface clearly, the balloon was sometimes filled with a contrast agent (iopamidol). The torsion-like movement of the left ventricle was not observed during the time-resolved x-ray recording. Sets of images with 66 frames/s (see below) were recorded every 0.20 mm horizontally along the equator of the heart.

X-ray diffraction technique

The experiments were made at the beamline BL40XU (Inoue et al., 2001) in the third-generation synchrotron radiation facility SPring-8 (Harima, Hyogo, Japan). The x-ray energy was 15.0 keV. The x-ray flux, which was reduced from the highest flux of 7×10^{14} photons/s by using an aluminum absorber, was ~2×10^{12} photons/s. The beam size (full width at half maximum) at the specimen was 0.25 mm horizontally, 0.10 mm vertically. The x-ray detector

was a beryllium-windowed x-ray image intensifier (V5445P, Hamamatsu Photonics, Hamamatsu, Japan; Amemiya et al., 1995) coupled to a fast CCD camera (C4880-80-24A, Hamamatsu Photonics). For studying diffraction from various parts of a heart, exposure time was 212 ms and 30–60 frames were recorded seamlessly while a heart was moving horizontally across the x-ray beam, as described above.

For recording images from a beating heart, the time resolution was 15 ms and 70 frames were recorded. A data acquisition system with an analog-to-digital converter was used to record the ventricular pressure, stimulus pulses, and the frame timing signal, which indicated the beginning of each frame. After the experiment, it was possible to correlate the cardiac cycle and the x-ray diffraction patterns. The sampling rate was 1 kHz.

For the data analysis, an x-ray diffraction pattern was divided into twelve 30° sectors around the direct beam. The vertical axis passed the top and bottom sectors in the middle (see frame 30 in Fig. 2). Since two opposite sectors are crystallographically equivalent (that is, the diffraction pattern is centrosymmetric), they were added together. Then, the equatorial intensity distribution in each sector was obtained by circularly averaging the intensity. The profile was fitted with a fourth-order polynomial function that simulated the background, and two Gaussian functions that simulated the (1,0) and (1,1) reflection peaks. The fitting was done by using a modified Levenberg-Marquardt algorithm (subroutine UNLSF in the IMSL library, Visual Numerics, San Ramon, CA). The intensity and position of a reflection were obtained from the area and center of the Gaussian function, respectively. The integrated intensity of the (1,1) reflection obtained this way is under-estimated by $\sqrt{3}$ compared to that of the (1,0) reflection, because the intensity is averaged, not summed, along an arc. Thus, the (1,1) intensity was multiplied by $\sqrt{3}$. Since the intensity of each equatorial reflection depends on the thickness of the sample, which changes considerably across a heart, the ratio of the intensities of the (1,0) and (1,1) reflections ($I(1,0):I(1,1)$) was used as an index of the equatorial intensity change.

The (1,0) lattice spacing ($d_{1,0}$) was obtained from the position of the (1,0) reflection. This is the separation of the (1,0) lattice planes and equal to $\sqrt{3}/2$ of the distance between centers of nearest thick filaments. The lattice spacing was calibrated using the 14.3-nm meridional reflection from frog skeletal muscle.

Since the energy bandwidth of the x-rays used in this study was ~2% (Inoue et al., 2001), the reflection peaks had a tail toward the higher angle. However, since the width of the equatorial reflections was much larger than the tail expected to arise from the bandwidth, no correction was made.

Definition of the axes and simulation of the equatorial reflections

The z axis runs from the apex to the base of the heart (Fig. 1). The y axis is parallel to the x-ray beam, which passes through the heart horizontally from anterior to posterior. The x axis is defined relative to the other two axes in a right-handed coordinate system. The x axis points from inside of the heart to the free wall of the left ventricle. The height where the heart is widest horizontally is taken as $z = 0$, which is called the ''equator.'' It should be noted that the x-ray equatorial reflections appear at right angles to the fiber axis, not in the direction of the equator of the heart.

At each part of the heart, the orientation of the muscle fiber was calculated from the model of the heart by Streeter et al. (1969) in diastole (Fig. 1), in which their angle relative to the z axis, measured from the x-y plane, changes continuously from ~$-60°$ at the epicardium to ~$+60°$ at the endocardium. Based on the model of arrangement of muscle fibers in a heart by Streeter et al. (1969), it is possible to predict the x-ray diffraction from each part of a heart. Muscle fibers run approximately parallel to the epicardium (Fig. 1). The direction of the fiber projected on the x-y (horizontal) plane follows the circumference of the heart. In addition to the free wall, two left ventricular papillary muscles were also included in the simulation. The axes of the papillary muscles were assumed to be vertical. Summing the contribution from all parts of the heart in the beam path gave diffraction from the heart. Absorption of x rays due to the ventricular wall
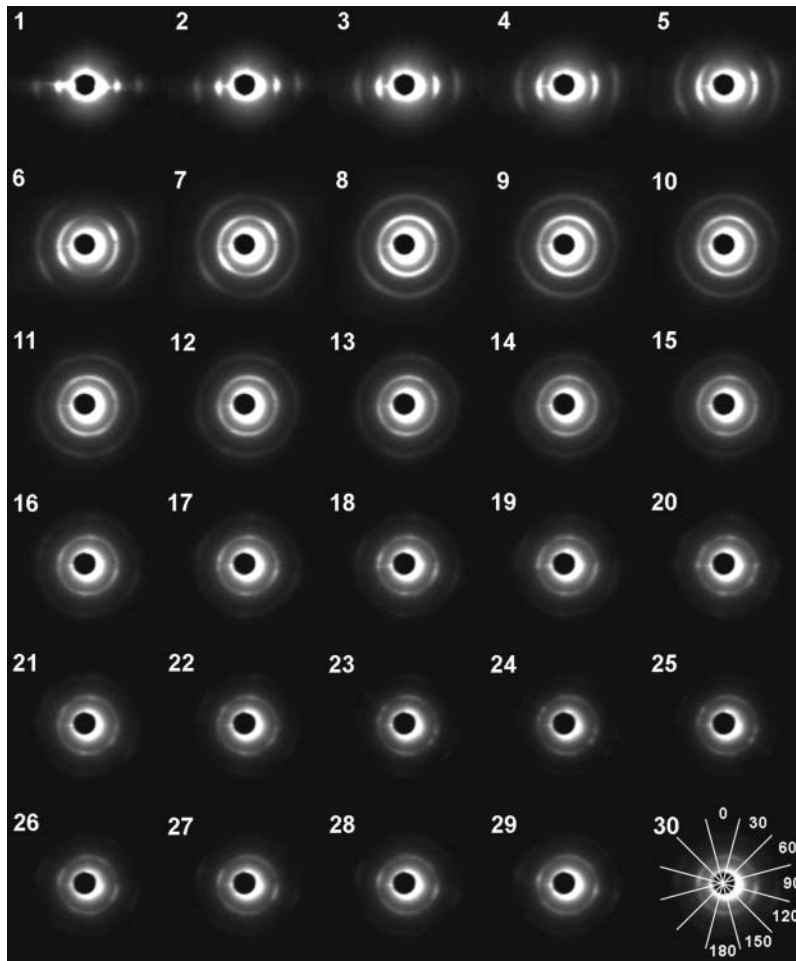
FIGURE 2 Diffraction patterns from various parts of an equatorial section of a rat heart. The heart moved by 0.21 mm in each frame so that the x-ray beam path is shifted from the epicardium (*1*) to the center (*30*). The central dark disk is the backstop with a central scatter around it. The inner arc/ring is the equatorial (1,0) reflection, the outer one the (1,1) reflection. In these images, the diffraction patterns are viewed from the downstream toward the upstream. In the last frame (*30*), the sectors that were used in the analysis of the diffraction pattern are shown. The number in each sector indicates the angle of the sector.

and the Tyrode solution in the left ventricle was taken into account by assuming an absorption coefficient of 0.755%/0.05 mm thickness (absorption of 15-keV x ray by water).

RESULTS

Changes in the x-ray diffraction diagram as the heart is scanned across

When the x-ray beam hit the edge of the left ventricular free wall, well-aligned (1,0) and (1,1) equatorial reflections were observed together with total reflection of x rays from the surface of the heart (Fig. 2, *frames 1–3*). When the beam penetrated into the free wall by 0.6 mm, the reflections became broader and formed arcs (*frames 4–5*). At the middle of the thickness of the free wall (at ∼1 mm from the surface), the arcs almost merged into circles (*frames 6–7*). There were two peaks along the arcs at ∼±45° from the horizontal. Further into the heart, the diffraction pattern became more circularly uniform with the top and bottom slightly enhanced (*frames 8–10*). When the beam passed through the anterior and posterior walls of the left ventricle, the diffraction pattern consisted of rings of the equatorial reflections with

emphasis at top and bottom (*frames 16–30*). In many cases, there were other sharp spots most often in the horizontal direction and also sometimes in oblique directions.

Theoretical considerations

The x-ray diffraction from a heart mostly consists of the (1,0) and (1,1) equatorial reflections (Fig. 3). These arise from the hexagonal arrangement of the thick and thin filaments in myofibrils. Although Fourier transform of a hexagonal lattice of filaments consists of hexagonally arranged diffraction spots in the equatorial plane, random azimuthal orientation of myofibrils makes the reflections circularly continuous and uniform in the reciprocal space. Due to the variation in the lattice spacing in different myofibrils, the reflections have an intrinsic width, which makes them tori in reciprocal space. The Ewald sphere has a radius of $1/\lambda$ (λ is the wavelength of the x-ray: 0.083 nm in the present experiment), but it can be approximated as a flat plane because the reflections treated here have Bragg spacing $<1/20$ nm^{-1}. When the muscle fiber is vertical (this is not realized in any part of the heart in Fig. 3 but is realized in
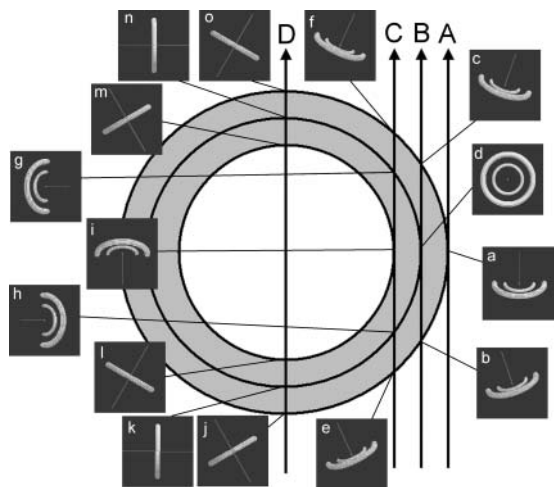
FIGURE 3 Schematic diagrams to show how the Fourier transform of the (1,0) and (1,1) reflections interacts with the Ewald sphere in reciprocal space. A cross section of the heart, seen from the top, is shown. At 15 representative points, the (1,0) and (1,1) equatorial reflections, which are two rings in reciprocal space, are calculated according to the fiber orientation predicted by the model of Streeter et al. (1969) and shown in the insets. The direction of the x-ray beam is normal to the drawing, passing at the center. The line in the insets is parallel to the fiber axis. The dark background of the insets is a part of the Ewald sphere, which cuts the rings of equatorial reflections. The cross sections of the rings by the Ewald sphere give rise to the equatorial reflections that we observe in an actual x-ray diffraction experiment. Depending on the orientation of the muscle fiber, the rings of the equatorial reflections change their orientation in the reciprocal space so that reflections are observed at different angles.
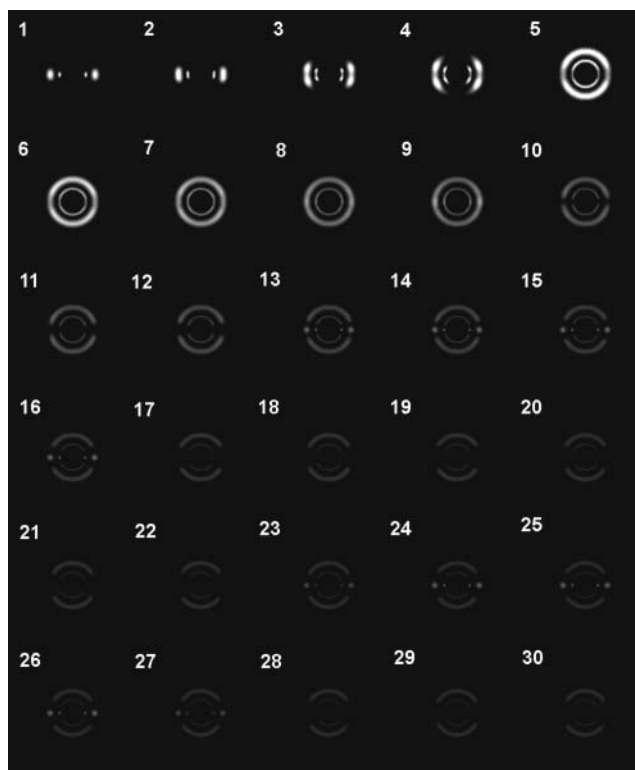

FIGURE 4 Calculated diffraction patterns when an x-ray beam passes through various parts of a rat heart. The x-ray beam path is shifted from the epicardium to the center of the heart by 0.21 mm every frame, just as in Fig. 2. The heart diameter was assumed to be 12 mm and the wall thickness 2 mm. The two papillary muscles with a diameter of 1.2 mm were assumed to be at 3.0 and 0.8 mm from the center of the heart, respectively, in the horizontal direction. The inner arc/ring is the (1,0) reflection, the outer one the (1,1) reflection. Note that the beam stop and the central scatter seen in Fig. 2 are absent in this simulation.

papillary muscles), its Fourier transform consists of two concentric circles in the horizontal (x-y) plane. A section of this Fourier transform by the Ewald sphere gives a diffraction pattern that consists of (1,0) and (1,1) spots on the equator on each side of the beam. These are the equatorial reflections observed in most x-ray diffraction experiments on striated muscle. However, in the present experiment, fibers are not necessarily at right angles to the x-ray beam.

When a heart is scanned by an x-ray beam from the side of the left ventricular free wall toward the center of the heart (Fig. 3, *arrow A*), the first part that the x-ray beam passes through is the epicardium of the free wall where the fibers run in the y-z plane. Although the fiber axis in the epicardium is tilted from the vertical (z) axis by ~30° (Streeter et al., 1969), the cross section of the Fourier transform by the Ewald sphere consists of only slightly oblique cross sections of the equatorial reflections, which are observed horizontally in the x-ray diffraction pattern (Fig. 3, *panel a*). Thus, when the beam hits the edge of the heart, which is the epicardium of the free wall, the diffraction is expected to consist of spots of the equatorial reflections in the horizontal direction (Fig. 4, *frame 1*). This is what was actually observed in the experiment from the epicardium (Fig. 2, *frames 1–3*).

When the beam passes deeper into the free wall, it traverses two epicardial surfaces in the anterior and posterior walls, and the layers of myocardium that are

within the wall. The projection of the fibers in the epicardial surface onto the horizontal (x-y) axis runs with an angle to the beam (Fig. 3, *arrow B*). Together with the tilt toward the z axis, this causes the equatorial reflections to become inclined from the horizontal direction. This inclination is opposite in surfaces in the anterior and posterior walls of the heart. Since the beam passed both surfaces, the diffraction pattern is symmetric across the vertical axis (Fig. 3, *panels b* and *c*). The deeper the fibers are in the free wall, the less inclined toward the z axis they are than in the surface. The fibers run in the horizontal plane at the middle of the thickness of the wall. In this case, as the fibers run parallel to the beam (the fibers are irradiated end-on; Fig. 3, *panel d*), the diffraction pattern consists of full circles (Iwamoto et al., 2002). Thus, when the beam moves from the epicardial surface to the center of the wall, the horizontal spots are split vertically to form arcs and move further up or down, and then the arcs become full circles (Fig. 4, *frames 3–7*). This is quite consistent with the observation (Fig. 2, *frames 5–8*).

When the beam passes through the endocardium (Fig. 3, *arrow C*), it travels through all layers of the wall. The fibers in the epicardial surfaces give the equatorial reflections obliquely (Fig. 3, *panels e and f*), whereas those at midwall, which are running in the horizontal plane, give reflections in the vertical direction (Fig. 3, *panels g and h*), and those in the endocardial surface, which are tilted toward the *z* axis but run parallel to the beam when projected onto the horizontal (*x-y*) plane, give reflections horizontally (Fig. 3, *panel i*). Thus, equatorial diffraction is observed in all directions (Fig. 4, *frames 8–9*). This also agrees well with the observation (Fig. 2, *frames 10–12*). The position of the endocardial surface was confirmed by filling the left ventricle with a contrast agent. In this case, the diffraction became very weak when the beam moved from the endocardial surface into the left ventricle cavity, making it easier to identify the position of the endocardium.

When the beam enters the left ventricle cavity and passes through the anterior and posterior walls (Fig. 3, *arrow D*), the diffraction pattern approaches a summation of those from fibers running approximately at right angles to the beam and with various vertical inclinations. The expected diffraction consists of arcs in vertical directions (Fig. 4, *frames 11–30*). Although this was actually observed in most hearts, strong spots of equatorial reflections were often found in this region of a heart (Fig. 2, *frames 16–30*). Origins of these strong reflections are probably the two major papillary muscles and other trabeculae, as shown in the simulation (Fig. 4, *frames 13–16 and 23–27*). Since fibers in these muscles are parallel to each other, diffraction from them is oriented and strong. The number, size and location of trabeculae vary considerably among hearts, but they mostly run vertically in the inner wall of the left ventricle so that their equatorial reflections tend to be observed in the horizontal direction. Since two trabeculae in the anterior and posterior walls may give reflections simultaneously, two sets of equatorial reflections may be observed.

In the strict sense, it is impossible to orient a heart ideally on an x-ray beam, with the beam at right angles to the *z* axis. When the heart is inclined around the *y* axis, the entire diffraction pattern is simply rotated around the x-ray beam. When it is tilted around the *x* axis, the whole diffraction pattern is affected. Practically, however, our simulation shows that as long as the rotation is much smaller than the tilt of fibers on the surface (~60°), the changes in the observed pattern are small.

Variation of lattice spacing in a heart

The equatorial lattice spacing was calculated from the peak position of the (1,0) reflection. According to the orientation of the muscle fibers, the reflection appeared in different angles and formed arcs or a ring (Fig. 2). Thus, the diffraction diagram was divided into twelve 30° sectors in such a way that the vertical line runs at the center of the top

and bottom sectors (Fig. 2, *frame 30*). Then, the intensity in each sector was averaged along an arc to obtain radial intensity distribution. The lattice spacing was measured only in the sectors where the (1,0) intensity was measurable. At the epicardium, the equatorial reflections were strong enough to be measured quantitatively only in the horizontal sector (Fig. 2, *frames 1–3*). When the x-ray beam passed through the middle of the wall (*arrow B* in Fig. 3) or the endocardium (*arrow C* in Fig. 3), the spacing was found to be ~37.5 nm on average (Fig. 5 *a*). This spacing was not different when
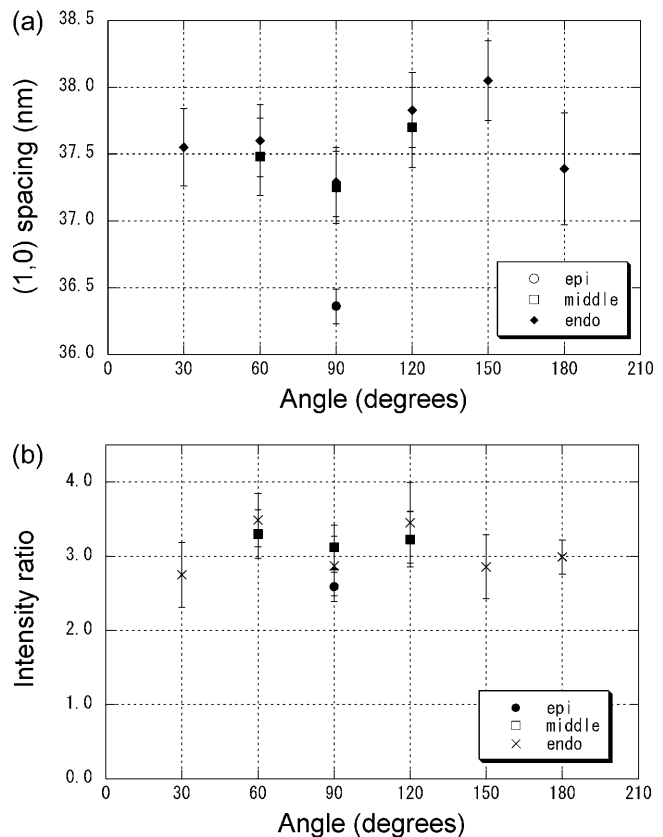

FIGURE 5 (*a*) The spacing of the equatorial (1,0) reflection arising in different directions when an x-ray beam passed through the epicardium, the middle of the free wall, and the endocardium of a rat heart. The angle of 90° corresponds to the horizontal, whereas 0° and 180° correspond to the vertical (see Fig. 2, *frame 30*). The mean value and the standard error of the mean in eight measurements are shown. When the x-ray beam passed through the epicardium (*arrow A* in Fig. 3), reflections were observed only horizontally (at 90°), whereas the reflections formed arcs when the beam passed through the middle of the wall (*arrow B* in Fig. 3), and the reflections were observed as full rings when the beam passed through the endocardium (*arrow C* in Fig. 3). At 90° the (1,0) spacing of epicardium was significantly smaller than those of middle and endocardium. No significant difference in lattice spacing was observed as a function of angle in the middle and endocardial regions. (*b*) The intensity ratio of the equatorial (1,0) and (1,1) reflections arising in different directions when the x-ray beam passed through the epicardium, the middle of the free wall, and the endocardium. The mean value and the standard error of the mean in eight measurements are shown. No significant difference in lattice spacing was observed as a function of angle in the middle and endocardial regions.

measured in different sectors. However, when the x-ray passed through the epicardium (*arrow A* in Fig. 3), the spacing was 36.4 nm, significantly smaller than in the same sector of the diffraction patterns from other parts ($p < 0.01$ in non-paired t-tests).

As discussed above, the sharp diffraction spots observed from the endocardium seem to arise from papillary muscles and trabeculae. The (1,0) lattice spacings of these reflections were also close to 37.5 nm.

Variation of the equatorial intensity ratio in a heart

The $I(1,0):I(1,1)$ ratio was also measured at three beam positions and different angles (Fig. 5 b). It was ~3.0, independent of the regions where the x-ray passed.

X-ray diffraction from a whole beating heart

In the present study, movement of a heart during a beat was reduced as much as possible by filling the left ventricle with a balloon and by encapsulating the heart in a plastic tube. To confirm the effectiveness of these methods, shift of the heart due to contraction was assessed by observing the diffraction from the epicardium surface. When the heart moved sideways due to contraction, diffraction recorded with an x-ray beam passing the surface appeared and disappeared because the heart moved in and out of the beam. In most experiments, this behavior was observed only at one or two beam positions when the beam was shifted by 0.22 mm horizontally. At other positions, the diffraction was either absent or always observed. Considering that the full width of the x-ray beam was ~0.4 mm, the movement of the heart was judged to be within this range. Thus, the contraction of the heart can be regarded as essentially isovolumic.

The intensities of the equatorial reflections were measured with the beam at three points, just below the epicardium surface, approximately at midwall, and in the endocardium region. Since the wall thickness was ~2 mm, these points were separated by ~0.6 mm. The measurement was made in a 30° sector where the reflections were the strongest. The time course of the change in the $I(1,0):I(1,1)$ ratio (Fig. 6 a) was similar in the three regions. It was an approximate mirror image of the time course of the left ventricular pressure (Fig. 6 b).

Changes in the peak position of the (1,0) reflection during contraction (results not shown) were more complicated in all regions. In some experiments, the peak shifted toward the larger angle, as expected from the lattice expansion due to muscle shortening. However, in many cases they moved toward the lower angle, or did not shift on contraction. This inconsistent behavior is considered to be caused by different contractility in different regions of the heart. Since myocardium is a continuous structure, different contractile force in different regions of the heart causes mutual stretching. A
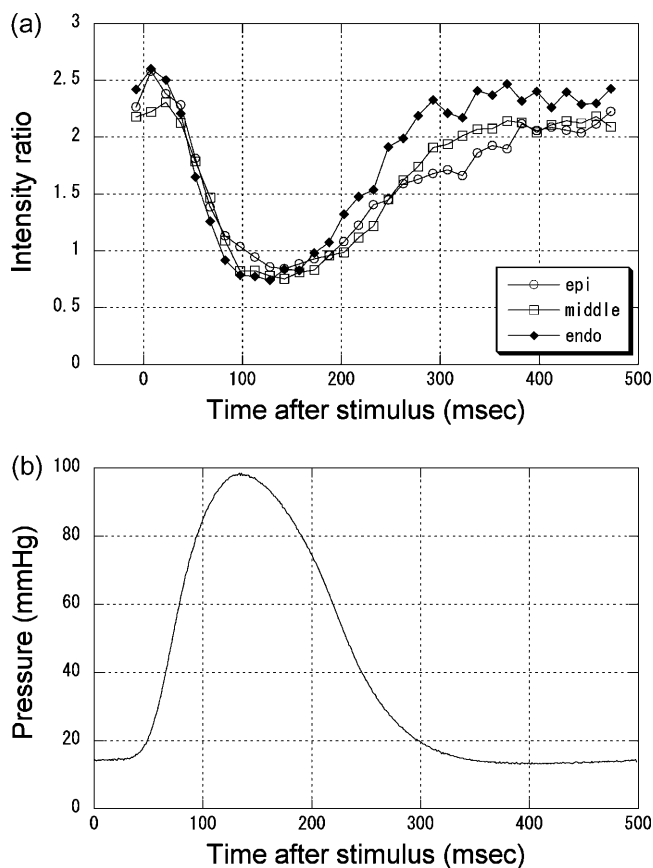

FIGURE 6 (*a*) Changes in the ratio of the intensities of the (1,0) and (1,1) equatorial reflections during contraction of a rat heart. Open circles are results obtained from the epicardium, open squares from the middle of the wall, and filled triangles from the endocardium. The data for the epicardium were obtained in the 90° sector, those for the midwall were in the 60° and 120° sectors, and those for endocardium were in the 180° sector. The three sets of data were averages of five contractions of four hearts. The standard error of the mean was 0.07–0.28 for the epicardium data, 0.03–0.15 for the midwall data, and 0.05–0.15 for the endocardium data. (*b*) Left ventricular pressure recorded during x-ray diffraction experiments. This is an average of all contractions used to record the data in Fig. 6 *a*.

region that develops larger force shortens by stretching other regions that produce smaller force. Thus, even in the isovolumic contraction, muscle fibers in different parts of the heart work under different conditions. This may be regarded as a limitation of the preparation used in the present experiment, in which movement due to contraction had to be restricted as much as possible to examine differences between various regions of the heart. In some cases, rings of equatorial reflections from the endocardium shrank in one direction and expanded in other directions during contraction. This clearly showed that different regions of the heart were giving rise to these reflections. However, in all experiments, the decrease in the equatorial intensity ratio shown in Fig. 6 *a* was observed, showing that the behavior of cross-bridges was not affected much by different loads on the muscle fiber.

The (1,0) spacing in diastole was, on average, 36.4 nm in the epicardium, and 37.5 nm in the middle of the wall and in the endocardium. Thus, they are not significantly different from the values obtained in quiescent hearts.

DISCUSSION

In this study, we found that equatorial reflections of the heart showed morphological changes such as horizontal spots, two pairs of horizontally directed arcs, two circles, and vertically directed arcs by scanning the heart from the epicardium of the left ventricular free wall toward the ventricular septum in a quiescent heart. Using a model, we revealed a relationship between the equatorial diffraction patterns and transmural fiber orientation from epicardium to endocardium. We also for the first time successfully observed myocardial cross-bridge dynamics in the beating heart. Variation of myofibril lattice spacing across the free wall was found in the end-diastolic phase. However, the dynamics of lattice changes were not well monitored in the present study due to the preparation of the specimen, and it has to be reinvestigated under more physiological conditions.

Assignment of the diffraction

Using the small x-ray beam available at the third-generation synchrotron radiation source, the x-ray diffraction patterns were recorded with x rays passing through different regions of the heart. It was found that the observed orientation of the equatorial reflections can be fundamentally explained by the reported model of the arrangement of muscle fibers in a heart (Streeter et al., 1969). However, close comparison between the observed (Fig. 2) and simulated (Fig. 4) diffraction patterns shows some differences. For instance, the beam must enter deeper into the wall from the epicardium to observe a circular pattern (Fig. 2, *frame 8*) than expected from the model (Fig. 4, *frame 5*). This may indicate that the orientation of muscle fibers does not change linearly with the depth in the wall, contrary to suggestions by Streeter et al. (1969). The depth in the wall at which fibers run in the horizontal plane seems closer to the endocardium than the epicardium.

Another unexpected observation was the presence of many diffraction spots when the x-ray beam was passing through the left ventricular cavity. This can be explained by the presence of papillary muscles and trabeculae on the surface of the endocardial wall. These reflections may be useful to monitor the contractility of the trabeculae and papillary muscles in an intact heart.

Generally speaking, although the x-ray diffraction patterns from a whole heart are more complicated than those from an isolated papillary muscle, it is possible to attribute features in the diffraction pattern to different regions of the heart. The most reliably assigned reflections are those which appear horizontally when the beam passes through the epicardium.

Since the x-ray beam in this case is not passing any muscle fibers other than those in the epicardium, the reflections can be assigned uniquely to them. Even without knowledge of where the x-ray beam is passing through, it is possible to recognize the equatorial reflections from the epicardium, which appear as well-oriented spots or arcs (Fig. 2, *frames 1–4*). Thus, analysis of the molecular changes in muscle fibers in the epicardium layer will be the most promising.

In other cases, the beam passes through more than one part of the heart, making the assignment more complex. However, when it is known where the x-ray beam is passing through, the layers giving the reflections may be identified by assuming a structural model of the heart, that is, by comparing Fig. 2 with Fig. 4. When it is not known where the beam is passing through, it is more difficult to assign reflections. When the beam traverses the region from the midwall to the ventricular cavity, full circles are observed in the diffraction pattern (Fig. 2, *frames 6–15*). However, when the beam is near the midwall, the intensity is stronger in the diagonal directions (*frames 6–7*), and when it is in the ventricular cavity, the intensity is higher in the vertical and horizontal directions (*frames 13–15*). The vertical component is from the free wall and the horizontal from trabeculae and papillary muscles. Thus, these regions can be identified from the diffraction pattern. Only in the area between these two regions (*frames 8–12*) does the intensity distribution stay similar. This area includes the inner layer of the free wall, the endocardial layer, and the cavity just above the endocardial surface. Since both the endocardium and the trabeculae give equatorial reflections in the horizontal direction, some intensity is continuously observed horizontally when the x-ray beam shifts from the endocardium to the ventricular cavity. In this region, precise attribution of the reflections to areas of the heart is difficult. To clearly define the beam position, contrast agent may help identify the endocardium by attenuating the x-ray beam in the cavity.

Lattice spacing and cross-bridge formation in cardiac muscles

The (1,0) lattice spacing of the fibers in the epicardium was found to be smaller by ~1 nm (Fig. 5 *a*) than that in other regions. Wherever the x-ray beam is, it always goes through the epicardium. However, the spacing was distinctly different when the beam was passing only through the epicardium. This suggests that only the top layer of the epicardium has a smaller lattice spacing. When the beam passed through other parts of the wall, the contribution from this thin layer is masked by those from the bulk of the wall, all fibers of which have a similar, larger lattice spacing.

In the expanded heart that was used in the present study, the myofilament lattice in most parts of the heart had a (1,0) spacing of ~37.5 nm and the epicardium top layer a spacing of 36.4 nm (Fig. 5 *a*). In our previous study on an isolated papillary muscle of the rat, it was found that the (1,0) spacing

was ~38.2 nm when the sarcomere length was 2.0 μm, and 37.2 nm when it was 2.15 μm (Yagi et al., 2004). Since the Tyrode solutions used in the present experiment and that on papillary muscles were of the same composition, the sarcomere length of the papillary muscle in the resting heart in the present study, which had a (1,0) spacing of 37.5 nm, may be 2.0–2.1 μm. Since the left ventricle was filled at the pressure of 10–20 mmHg in our preparation, this should be taken as the spacing in the end-diastolic state of contraction. The difference in the (1,0) spacings in the top epicardium layer and the rest of the heart may indicate that sarcomere lengths in those regions are different. However, since the cell volume itself may be different, this conclusion is not decisive. Although the smaller lattice spacing suggests longer sarcomere length in the epicardium, previous reports (summarized by Streeter and Hanna, 1973) showed no such tendency in the diastolic state.

Although the (1,0) spacing was not homogenous, the $I(1,0):I(1,1)$ ratio was found to be constant in the entire wall (Fig. 4 b). The observed ratio of ~3 is similar to that which we usually observe in an isolated papillary muscle in a quiescent state with a similar lattice spacing (lattice spacing can be changed by changing the muscle length). Thus, the isolated papillary muscle preparation seems to retain the characteristics it has in a heart.

When recorded during contraction, the $I(1,0):I(1,1)$ ratio was ~2.5 in diastole and 0.8 in systole, regardless of the region of the heart (Fig. 6 a). The diastolic ratio is not significantly different from that observed in quiescent hearts (Fig. 5 b). The (1,0) spacing was also similar. Thus, the diastolic state of the heart muscle was similar to the quiescent state. This is in contrast to the results obtained in canine papillary muscle (Matsubara, 1980), which showed a lower ratio in diastole than in the quiescent state. The difference may be due to the slow rate of beating in the present study. Although the frequency of 2 Hz was comparable to that used in the experiments on canine muscle, it is very slow considering the physiological heart rate of a rat, which is in the range of 5–7 Hz.

The systolic $I(1,0):I(1,1)$ ratio of 0.8, which was observed in the present study, is similar to that obtained in experiments on isolated papillary muscles of various species (Matsubara, 1980, on canine heart; Matsubara et al., 1989, on rat heart; Yagi et al., 2001, on ferret heart). It is known in canine papillary muscle that the ratio is smaller when the developed tension is enhanced by raising the heart rate (Matsubara, 1980). Thus, the ratio is related to the formation of myosin cross-bridges in muscle contraction (Haselgrove and Huxley, 1973). The decrease during contraction observed in the present study indicates that a significant number of cross-bridges, which is comparable to that formed in an isolated papillary muscle in contraction, is formed in the ventricular wall muscle of a whole heart. Although the intensity ratio from the endocardium appears to return to the diastolic level faster than those in other

regions, the results were not consistently observed, probably because of the problem of the preparation as discussed above. This should be studied further in a heart under a more physiological condition.

In conclusion, we demonstrated that the x-ray equatorial diffraction pattern from a whole heart can be interpreted based on the structural model of the arrangement of muscle fibers in a heart. A significant activity of myosin cross-bridges was confirmed in a beating heart. These results show that x-ray diffraction studies on a whole heart can be a powerful tool to investigate the activity of myosin molecules in cardiac muscle cells. Although the heart was held static in the present study, it is necessary to allow pumping to study a heart in a physiological state. Since the diffraction patterns from most parts of a heart are distinguishably different, it is possible to assign the origin of observed diffraction in each frame of time-resolved recording even when the heart moves in the beam. By combining a number of results obtained with an x-ray beam passing through different regions of the heart, it will be possible to investigate the behavior of the muscles in all regions of the heart during contraction. Currently, studies are in progress to investigate the behavior of myosin cross-bridges in a whole heart under a more physiological condition. This technique can be also used on hearts under pathological conditions to elucidate the molecular basis of cardiac diseases.

REFERENCES

Amemiya, Y., K. Ito, N. Yagi, Y. Asano, K. Wakabayashi, T. Ueki, and T. Endo. 1995. Large-aperture TV detector with a beryllium-windowed image intensifier for x-ray diffraction. *Rev. Sci. Instrum.* 66: 2290–2294.

Haselgrove, J. C., and H. E. Huxley. 1973. X-ray evidence for radial cross-bridge movement and for the sliding filament model in actively contracting skeletal muscle. *J. Mol. Biol.* 77:549–568.

Hooks, D. A., K. A. Tomlinson, S. G. Marsden, I. J. LeGrice, B. H. Smaill, A. J. Pullan, and P. J. Hunter. 2002. Cardiac microstructure: implications for electrical propagation and defibrillation in the heart. *Circ. Res.* 91:331–338.

Hsu, E. W., A. L. Muzikant, S. A. Matulevicius, R. C. Penland, and C. S. Henriquez. 1998. Magnetic resonance myocardial fiber-orientation mapping with direct histological correlation. *Am. J. Physiol.* 274: H1627–H1634.

Inoue, K., T. Oka, T. Suzuki, N. Yagi, K. Takeshita, S. Goto, and T. Ishikawa. 2001. Present status of high flux beamline (BL40XU) at SPring-8. *Nucl. Instrum. Methods Phys. Res.* A467–468:674–677.

Iwamoto, H., Y. Nishikawa, J. Wakayama, and T. Fujisawa. 2002. Direct visualization of a single hexagonal myofilament lattice in native myofibrils of striated muscle by x-ray diffraction. *Biophys. J.* 83:1074–1081.

Matsubara, I. 1980. X-ray diffraction studies on the heart. *Annu. Rev. Biophys. Bioeng.* 9:81–105.

Matsubara, I., N. Yagi, D. W. Maughan, Y. Saeki, and Y. Amemiya. 1989. X-ray diffraction study on heart muscle during contraction. *In* Muscle Energetics. R. J. Paul, G. Elzinga, and K. Yamada, editors. Alan R. Liss, New York. 481–486.

Sowerby, A. J., J. Harries, G. P. Diakun, E. Towns-Andrews, J. Bordas, and A. Stier. 1994. X-ray diffraction studies of whole rat heart during anoxic perfusion. *Biochem. Biophys. Res. Commun.* 202:1244–1251.

Streeter, D. D., Jr., and W. T. Hanna. 1973. Engineering mechanics for successive states in canine left ventricular myocardium. II. Fiber angle and sarcomere length. *Circ. Res.* 33:656–664.

Streeter, D. D., Jr., H. M. Spotnitz, D. P. Patel, J. Ross, and E. H. Sonnenblick. 1969. Fiber orientation in the canine left ventricle during diastole and systole. *Circ. Res.* 24:339–347.

Yagi, N., H. Okuyama, H. Toyota, J. Araki, J. Shimizu, G. Iribe, K. Nakamura, S. Mohri, K. Tsujioka, J. Suga, and F. Kajiya. 2004. Sarcomere-length dependence of latice volume and radial mass transfer of myosin cross-bridges in rat papillary muscle. *Pflugers Arch. Eur. J. Physiol.* In press.

Yagi, N., Y. Saeki, T. Ishikawa, and S. Kurihara. 2001. Cross-bridge and calcium behavior in ferret papillary muscle in different thyroid states. *Jpn. J. Physiol.* 51:319–326.